Anion Transport with Pnictogen Bonds in Direct Comparison with Chalcogen and Halogen Bonds

Lee, Lucia M.; Tsemperouli, Maria; Poblador Bahamonde, Amalia Isabel; Benz, Sebastian; Sakai, Naomi; Sugihara, Kaori; Matile, Stefan

How to cite

LEE, Lucia M. et al. Anion Transport with Pnictogen Bonds in Direct Comparison with Chalcogen and Halogen Bonds. In: Journal of the American Chemical Society, 2019, vol. 141, n° 2, p. 810–814. doi: 10.1021/jacs.8b12554

This publication URL: https://archive-ouverte.unige.ch/unige:113057

Publication DOI: 10.1021/jacs.8b12554

Anion Transport with Pnictogen Bonds in Direct Comparison with Chalcogen and Halogen Bonds

Lucia M. Lee,‡ Maria Tsemperouli,‡ Amalia I. Poblador-Bahamonde, Sebastian Benz, Naomi Sakai, Kaori Sugihara,* and Stefan Matile*

School of Chemistry and Biochemistry, NCCR Chemical Biology, University of Geneva, CH-1211 Geneva, Switzerland

‡These two authors contributed equally

ABSTRACT. In this communication, we introduce transmembrane anion transport with pnictogen-bonding compounds and compare their characteristics with chalcogen- and halogen-bonding analogs. Tellurium-centered chalcogen bonds are at least as active as antimony-centered pnictogen bonds, whereas iodine-centered halogen bonds are three orders of magnitude less active. Irregular, voltage-dependent single-channel currents, high gating charges, efficient dye leakage and small Hill coefficients support the formation of bulky, membrane-disruptive supramolecular amphiphiles by tris(perfluorophenyl)stibanes that bind anions "too strongly." In contrast, the chalcogen-bonding bis(perfluorophenyl)tellanes do not cause leakage and excel as carriers with nanomolar activity, $P_{(Cl/Na)} = 10.4$ for anion/cation selectivity and $P_{(Cl/NO3)} = 4.5$ for anion selectivity. Selectivities are lower with pnictogen-bonding carriers because their membrane-disturbing 3D structure affects also weaker binders ($P_{(Cl/Na)} = 2.1$, $P_{(Cl/NO3)} = 2.5$). Their 2D structure, directionality, hydrophobicity and support from proximal anion-π interactions are suggested to contribute to the unique power of chalcogen bonds to transport anions across lipid bilayer membranes.

The integration of unorthodox interactions into functional systems is of fundamental importance because it promises access to new activities.[1] Synthetic transport systems[2] have emerged as an attractive tool to assess the functional relevance of such interactions. Realized examples include anion-π interactions in many variations,[1] halogen bonds[3,4] and, more recently, also chalcogen bonds.[5,6] In the following, we elaborate on anion transport with pnictogen bonds in direct comparison to chalcogen and halogen bonds. These so-called σ-hole interactions[7,8] originate from highly localized areas of highly positive charge density that appear on heavier and p-block elements. Associated with σ* orbitals, the σ holes appear at the opposite side of the covalent bonds and deepen with increasing electron deficiency of the atom. As a result, there is one σ hole available per atom for halogen bonds,[9] two for chalcogen,[10] three for pnictogen[11,12] and four for tetrel bonds (Figure 1).[7,8] Increasing with polarizability, the depth of the σ holes

increases from top to bottom and from right to left in the periodic table (Table 1, entry 2).[7,8,11] With tetrel bonds suffering from overcrowding, pnictogen bonds in general and antimony in particular emerged as most promising for the integration into functional systems.[11]

We have already reported the synthesis, chloride binding in theory and experiment, and catalytic activity of compounds **1**-**7** (Figures 1,2).[11] Ion transport was explored first in planar or "black" lipid bilayers (BLMs).[2-5] The addition of 200 μM bis(perfluorophenyl)tellane **4** to 1-palmitoyl-2-oleoyl-*sn*-3-phosphatidylcholine (POPC) BLMs and the application of voltage caused the appearance of macroscopic currents without resolved single-channel on-off steps, thus supporting that tellanes **4** function as ion carriers (Figure 2C).[3,6,13] The *I*-*V* curve showed non-ohmic behavior

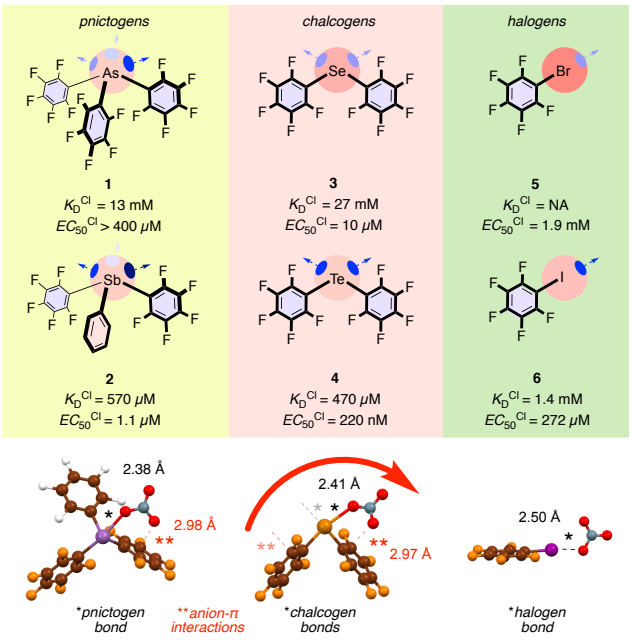

Figure 1. Candidates tested for anion transport with pnictogen, chalcogen and halogen bonds, with K_D's for Cl binding,[11] EC_{50}'s for anion transport, and M06-2X/6–311G**/aug-cc-pVTZ structures of nitrate complexes of **2**, **4** and **6** (red arrow: Possible anion slide).

characterized by a formal gating charge of $z_g = 0.72 \pm 0.06$ (Figure 2A).[3,13] With perfluorinated systems, z_g increased with increasing depth of the σ holes (**7**>**4**>**6**, Table 1, entry 3).

The application of NaCl gradients across the BLMs resulted in different currents at negative and positive voltages (Figures 2A,C). A positive reversal potential V_r = +14.5 mV, i.e., the potential needed to stop spontaneous "zero" current from flowing along the salt gradient, demonstrated that carriers **4** are anion selective (Table S1). GHK analysis gave an anion/cation permeability ratio $P_{Cl/Na}$ = 10.4 (Table 1, entry 4). The same procedure applied to a chloride/nitrate gradient with 2 M NaCl and $NaNO_3$ in *cis* and *trans*

chamber, respectively, gave an anion/anion permeability ratio $P_{Cl/NO3}$ = 4.5 (entry 5, Figure 2B○). Chloride was also preferred over perchlorate ($P_{Cl/ClO4}$ = 1.8) and sulfate ($P_{Cl/SO4}$ = 8.3, Figures 2B□●,S17). The anion/cation and anion/anion selectivities found with chalcogen bonds in **4** decreased with halogen bonds in **6** and even more with pnictogen bonds in **2** (entries 4,5). The less activated stibane **2** was used instead of the most powerful pnictogen-bond donor **7**, because the latter produced irregular bursts in conductance experiments (Figure 2D,E). The randomly varying channel-like currents in these bursts suggested that stibane **7** disturbs the membrane order by forming transient, large and disordered pores (Figure 2E).

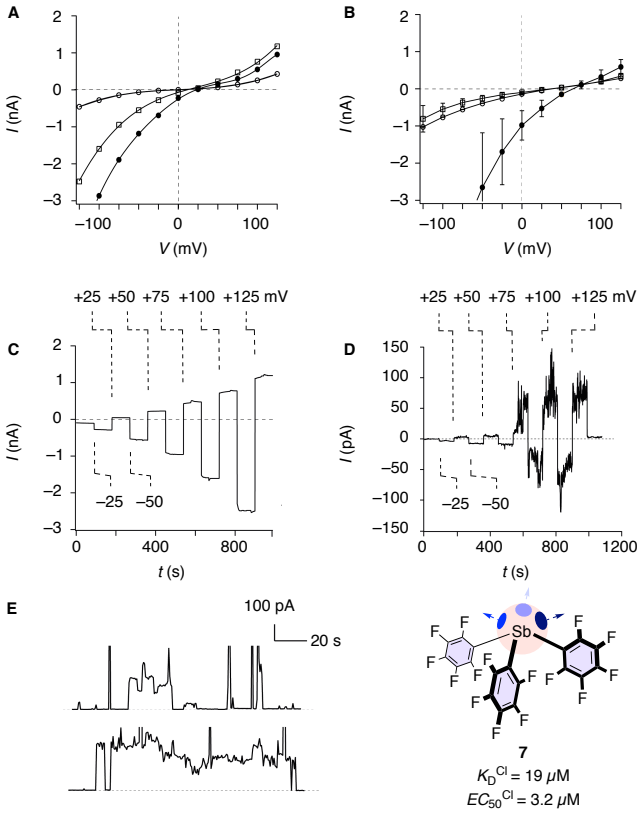

Figure 2. Ion transport characteristics of **4** and **7** in BLM conductance measurements. (A) *I-V* profile of **4** with 2 M NaCl *cis* and 2 M (○), 1 M (□) or 0.5 M NaCl *trans* (●). (B) Same with 2 M $NaNO_3$ (○), 2 M $NaClO_4$ (□) or 1 M Na_2SO_4 *trans* (●). (C) Macroscopic current of **4** with 2 M NaCl *cis* and 1 M *trans* with increasing voltage *V*. (D) Same for **7** with 2 M NaCl *cis* and *trans*. (E) Same for **7** at 200 mV time-resolved for channel-like currents, with structure, K_D for Cl binding[11] and EC_{50} for transport.

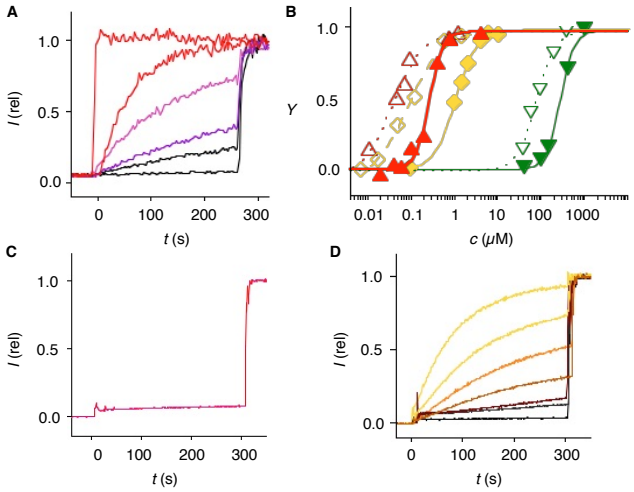

Figure 3. (A, B) Anion transport of **2** (◆◇), **4** (▲△, A) and **6** (▼▽) and (C, D) dye leakage of **4** (C) and **7** (D). (A) Change in ratiometric emission (λ_{em} = 510 nm; λ_{ex1} = 404 nm, λ_{ex2} = 454 nm) upon addition of **4** (0 (black) to 2.0 μM (red); ~0 s) and excess gramicidin D (260 s) to EYPC vesicles with internal HPTS, a pH gradient, and 100 mM internal and external NaCl. (B) Dependence of the fractional activity *Y* in the HPTS assay (A) on the concentration of **2** (◆◇), **4** (▲△) and **6** (▼▽) in the absence (◆▲▼) and presence (◇△▽) of FCCP (1 μM), with fit to Hill equation). (C) Change in emission (λ_{em} = 517 nm; λ_{ex} = 492 nm) upon addition of **4** (1 mM, 0 s) and excess triton X100 to POPC vesicles with internal CF. (D) Same for **7** (0 (black), 4, 8, 20, 40, 80, 100 μM (gold)).

Transport activity in large unilamellar vesicles (LUVs) was determined with the HPTS assay (Figure 3).[3,13,14] LUVs composed of egg yolk phosphatidylcholine (EYPC) were loaded with the ratiometric pH probe HPTS and exposed to a pH gradient. The dissipation of this gradient in response to the addition of carrier **4** was then followed over time until completion after the addition of excess gramicidin D (Figure 3A). The fractional activities *Y* were then plotted against the concentration of the carrier and fitted to the Hill equation (Figure 3B▲). The $EC_{50}^{Cl} = 200 \pm 20$ nM obtained for chalcogen-bonding carrier **4** revealed outstanding activity, particularly considering the simplicity of the structure (Table 1, entry 6).[15] Halogen-bonding homologs **6** were already known[3] to be three orders of magnitude less active. In clear contrast, pnictogen-bonding carrier **2** and detergent **7** were not much more but even slightly less active than tellane **4** (Figure 3B◆▼, entry 6; (pentafluorophenyl)diphenylstibane was less active than **2**; i.e., EC_{50} = 2.9 μM).

Replacement of extravesicular chlorides by nitrates decreased the activity of all transporters without change of the Te>Sb>I sequence (entry 8). These results were consistent with the $P_{Cl/NO3}$ obtained in BLM experiments (entries 5,10). In the presence of the proton carrier FCCP at concentrations that do not cause activity alone, the activity of all carriers increased (entry 11). This trend supported that, in the

HPTS assay, anion/hydroxide antiport dominates without FCCP and coupled anion/proton symport with FCCP.[13,14] Preserved Te>Sb>I activity and Cl>NO_3 selectivity with FCCP (entries 11,12) and decreasing activity in increasingly charged EYPC/EYPG membranes (entry 24) confirmed that σ-hole interactions with anions dominate carrier activity.

Table 1. Characteristics of Anion Transporters.

Entry	Characteristics[a-l]	Carriers[m-p]			
		7[n]	**2**	**4**	**6**
1	Element[a]	Sb	Sb	Te	I
2	α^b	43	43	38	32
3	$z_g{}^c$	0.9	0.4	0.7	0.4
4	$P_{Cl/Na}{}^d$		2.1	10.4	5.0
5	$P_{Cl/NO3}{}^d$		2.5	4.5	3.3
6	$EC_{50}{}^{Cl}$ (μM)[e]	3.2	1.0	0.2	272[o]
7	n^f	1.5	2.3	1.9	2.7[o]
8	$EC_{50}{}^{NO3}$ (μM)[e]		2.2	0.8	459
9	n^f		0.9	4.6	1.2
10	$EC_{50}{}^{NO3}$ / $EC_{50}{}^{Cl}$ [g]		2.2	4.0	1.7
11	$EC_{50}{}^{Cl,FCCP}$ (μM)[h]		0.05	0.03	80
12	$EC_{50}{}^{NO3,FCCP}$ (μM)[h]		0.2	0.06	119
13	$K_D{}^{Cl}$ (mM)[i]	0.02[t]	0.6[p]	0.5[p]	1.4[p]
14	$E_{int}{}^{Cl}$ (kcal mol^{-1})[j]	–52[p]	–44[p]	–40[p]	–28[p]
15	$E_{int}{}^{NO3}$ (kcal mol^{-1})[j]	–48	–43	–35	–23
16	$EC_{50}{}^{Br}$ (μM)[e]			0.4	256
17	$EC_{50}{}^{I}$ (μM)[e]			0.6	379
18	$EC_{50}{}^{Br,FCCP}$ (μM)[h]			0.03	143
19	$EC_{50}{}^{I,FCCP}$ (μM)[h]			0.03	338
20	$K_D{}^{Br}$ (mM)[i]			1.7	2.0
21	$K_D{}^{I}$ (mM)[i]			4.3	6.3
22	$E_{int}{}^{Br}$ (kcal mol^{-1})[j]			–35	–24
23	$E_{int}{}^{I}$ (kcal mol^{-1})[j]			–30	–21
24	$EC_{50}{}^{Cl}$ (10% PG) (μM)[k]		7.8	1.2	575
25	$EC_{50}{}^{CF}$ (μM)[l]	43	>10^4	>10^4	>10^4

[a]Donors for σ-hole interactions in carriers. [b]Computed polarizabilities of elements based on MP2 calculations (a.u.).[6] [c]Formal gating charge, from *I-V* curves in BLMs (Figure 2). [d]Permeability ratios in BLMs, from GHK equation applied to V_r with NaCl (2 M *cis*, 1 M *trans*) or NaCl/$NaNO_3$ gradients (Figures 2, S16-S18). [e]Effective concentration to reach 50% of maximal activity in the HPTS assay with internal NaCl and variable external anions (NaX, EYPC LUVs, Figures 3A, B, S6-S10). [f]Hill coefficient. [g]Anion selectivity ratio according to the HPTS assay. [h]As in *e* with FCCP (1 μM). [i]Dissociation constants from NMR titrations with TBAX in THF-d_8 (X = Cl, Br, I). [j]Interaction energies for 1:1 complexes computed at M06-2X/6–311G**/aug-cc-pVTZ level. [k]As in *e* with EYPC/EYPG 9:1 LUVs. [l]Effective concentration to reach 50% of maximal activity in the CF assay (NaCl, POPC LUVs, Figure S15). [m]See Figure 1 for structures. [n]Selected pertinent data because of different mode of action (Figures 2D, 2E, 3D). [o,p]Data from refs 3[o] and 11,[p] in part remeasured.

Anion binding studies in THF and computed binding energies of 1:1 complexes were in good agreement with the anion selectivities found for transport ($Cl>NO_3$, Cl>Br>I, entries 13-23). The computed chalcogen- and pnictogen-bonding complexes with nitrate were particularly interesting because besides the dominant σ-hole interactions, they also showed strong edge-to-face nitrate-π interactions[16] with one of the adjacent pentafluorophenyl rings (Figure 1). Their absence in the underperforming halogen bonds implied special importance of these coupled chalcogen(pnictogen)/anion–π "slides" for anion translocation.

In general, these results supported that increasing stability of anion complexes with increasing depth of the σ holes chiefly determines the transport characteristics. Increasing gating charges z_g, i.e. current rectification,[3,13] with deepening σ holes in **7**>**4**>**6** (pnictogen>chalcogen>halogen) were well explained with increasingly stable anion complexes (entry 3). For chalcogen bonds in **4** compared to halogen bonds in **6**, increasingly stable anion complexes also explained the increase in activity and selectivity convincingly (**4**>**6**, entries 4-6,8,10). With pnictogen bonds, however, the consequences of increasingly stable anion complexes were different. Anion binding produced supramolecular 3D amphiphiles[17] that with increasing stability increasingly disturbed membrane organization. At maximal stability of the anion complexes with **7**, the result were transient, large and disordered pores. They were clearly detected in conductance experiments (Figure 2D) and from dye leakage in the CF assay (Figure 3D, contrary to all other carriers, including **4**, Figure 3C). Increasing membrane disorganization caused by 3D pnictogen-bonding amphiphiles already before bilayer rupture was reflected in decreasing anion selectivity (**2**<**4**, entries 4,5,10) and decreasing activity (**2**<**4**, **1**<<**3**, Figure 1) compared to the respective membrane-matching 2D chalcogen-bond donors. Although these interpretations were remarkably consistent throughout a series of independent experiments, the possible influence of other contributions should not be underestimated. These include differences in partitioning, differences in fluorophilicity to enhance detergent effects of **7**, or, less likely, that decomposition of **7** causes membrane disorder.

In summary, these results explicitly introduce pnictogen bonds to ion transport and disclose bis(perfluorophenyl)tellane as a very powerful anion carrier for its size. Chalcogen bonds outperforming pnictogen bonds for transport is contrary to expectations from binding and catalysis. The availability of two in-plane σ holes with adjacent π-acidic surfaces for secondary anion-π interactions could account for the high activity and selectivity of tellane **4** (Figure 1). The significant differences found between halogen, chalcogen and pnictogen bonds confirm that their directionality and hydrophobicity, exceeding all conventional interactions – also hydrogen-bond donors, by far –, provides access to new levels of precision on the molecular level. Their integration into functional systems deserves high attention for this reason.

ASSOCIATED CONTENT

Supporting Information. Detailed experimental procedures. This material is available free of charge via the Internet at http://pubs.acs.org.

AUTHOR INFORMATION

Corresponding Author

stefan.matile@unige.ch, kaori.sugihara@unige.ch

Notes

The authors declare no competing financial interest.

ACKNOWLEDGMENTS

We thank the NMR and the MS platforms for services, and the University of Geneva, the Swiss National Centre of Competence in Research (NCCR) Chemical Biology, the NCCR Molecular Systems Engineering and the Swiss NSF for financial support.

REFERENCES

(1) Zhao, Y.; Cotelle, Y.; Sakai, N.; Matile, S. Unorthodox Interactions at Work. *J. Am. Chem. Soc.* **2016**, *138*, 4270–4277.

(2) (a) Muraoka, T.; Umetsu, K.; Tabata, K. V.; Hamada, T.; Noji, H.; Yamashita, T.; Kinbara, K. Mechano-Sensitive Synthetic Ion Channels. *J. Am. Chem. Soc.* **2017**, *139*, 18016–18023. (b) Schneider, S.; Licsandru, E. D.; Kocsis, I.; Gilles, A.; Dumitru, F.; Moulin, E.; Tan, J.; Lehn, J. M.; Giuseppone, N.; Barboiu, M. Columnar Self-Assemblies of Triarylamines as Scaffolds for Artificial Biomimetic Channels for Ion and for Water Transport. *J. Am. Chem. Soc.* **2017**, *139*, 3721–3727. (c) Shinde, S. V.; Talukdar, P. A Dimeric Bis(melamine)-Substituted Bispidine for Efficient Transmembrane H(+)/Cl(-) Cotransport. *Angew. Chem. Int. Ed.* **2017**, *56*, 4238–4242. (d) Kempf, J.; Schmitzer, A. R. Metal-Organic Synthetic Transporters (MOST): Efficient Chloride and Antibiotic Transmembrane Transporters. *Chem. Eur. J.* **2017**, *23*, 6441–6451. (e) Su, G.; Zhang, M.; Si, W.; Li, Z.-T.; Hou, J.-L. Directional Potassium Transport through a Unimolecular Peptide Channel. *Angew. Chem. Int. Ed.* **2016**, *55*, 14678–14682. (f) Jones, J. E.; Diemer, V.; Adam, C.; Raftery, J.; Ruscoe, R. E.; Sengel, J. T.; Wallace, M. I.; Bader, A.; Cockroft, S. L.; Clayden, J.; Webb, S. J. Length-Dependent Formation of Transmembrane Pores by 3_{10}-Helical alpha-Aminoisobutyric Acid Foldamers. *J. Am. Chem. Soc.* **2016**, *138*, 688–695. (g) Wei, X.; Zhang, G.; Shen, Y.; Zhong, Y.; Liu, R.; Yang, N.; Al-Mkhaizim, F. Y.; Kline, M. A.; He, L.; Li, M.; Lu, Z.-L.; Shao, Z.; Gong, B. Persistent Organic Nanopores Amenable to Structural and Functional Tuning. *J. Am.*

Chem. Soc. **2016**, *138*, 2749–2754. (h) Lisbjerg, M.; Valkenier, H.; Jessen, B. M.; Al-Kerdi, H.; Davis, A. P.; Pittelkow, M. Biotin[6]uril Esters: Chloride-Selective Transmembrane Anion Carriers Employing C-H...Anion Interactions. *J. Am. Chem. Soc.* **2015**, *137*, 4948–4951. (i) Montenegro, J.; Ghadiri, M. R.; Granja, J. R. Ion Channel Models Based on Self-Assembling Cyclic Peptide Nanotubes. *Acc. Chem. Res.* **2013**, *46*, 2955–2965. (j) Otis, F.; Auger, M.; Voyer, N. Exploiting Peptide Nanostructures to Construct Functional Artificial Ion Channels. *Acc. Chem. Res.* **2013**, *46*, 2934–2943. (k) Davis, J. T.; Okunola, O.; Quesada, R. Recent Advances in the Transmembrane Transport of Anions. *Chem. Soc. Rev.* **2010**, *39*, 3843–3862. (l) Hagihara, S.; Tanaka, H.; Matile, S. Boronic Acid Converters for Reactive Hydrazide Amplifiers: Polyphenol Sensing in Green Tea with Synthetic Pores. *J. Am. Chem. Soc.* **2008**, *130*, 5656–5657. (m) Goto, C.; Yamamura, M.; Satake, A.; Kobuke, Y. Artificial Ion Channels Showing Rectified Current Behavior. *J. Am. Chem. Soc.* **2001**, *123*, 12152–12159. (n) Baumeister, B.; Sakai, N.; Matile, S. p-Octiphenyl β-Barrels with Ion Channel and Esterase Activity. *Org. Lett.* **2001**, *3*, 4229–4232. (o) Fyles, T. M.; Loock, D.; Zhou, X. A Voltage-Gated Ion Channel Based on a Bis-Macrocyclic Bolaamphiphile. *J. Am. Chem. Soc.* **1998**, *120*, 2997–3003.

(3) Vargas Jentzsch, A.; Emery, D.; Mareda, J.; Nayak, S. K.; Metrangolo, P.; Resnati, G.; Sakai, N.; Matile, S. Transmembrane Anion Transport Mediated by Halogen-Bond Donors. *Nat. Commun.* **2012**, *3*, 905.

(4) Ren, C.; Ding, X.; Roy, A.; Shen, J.; Zhou, S.; Chen, F.; Yau Li, S. F.; Ren, H.; Yang, Y. Y.; Zeng, H. A Halogen Bond-Mediated Highly Active Artificial Chloride Channel with High Anticancer Activity. *Chem. Sci.* **2018**, *9*, 4044–4051.

(5) Benz, S.; Macchione, M.; Verolet, Q.; Mareda, J.; Sakai, N.; Matile, S. Anion Transport with Chalcogen Bonds. *J. Am. Chem. Soc.* **2016**, *138*, 9093–9096.

(6) Macchione, M.; Tsemperouli, M.; Goujon, A.; Mallia, A. R.; Sakai, N.; Sugihara, K.; Matile, S. Mechanosensitive Oligodithienothiophenes: Transmembrane Anion Transport Along Chalcogen-Bonding Cascades. *Helv. Chim. Acta* **2018**, *101*, e1800014.

(7) Bauza, A.; Mooibroek, T. J.; Frontera, A. The Bright Future of Unconventional Sigma/pi-Hole Interactions. *ChemPhysChem* **2015**, *16*, 2496–2517.

(8) Lim, J. Y. C.; Beer, P. D. Sigma-Hole Interactions in Anion Recognition. *Chem* **2018**, *4*, 731–783.

(9) Cavallo, G.; Metrangolo, P.; Milani, R.; Pilati, T.; Priimagi, A.; Resnati, G.; Terraneo, G. The Halogen Bond. *Chem. Rev.* **2016**, *116*, 2478–2601.

(10) (a) Vogel, L.; Wonner, P.; Huber, S. M. Chalcogen Bonding: An Overview. *Angew. Chem. Int. Ed.*, in press, doi: 10.1002/anie.201809432. (b) Mahmudov, K. T.; Kopylovich, M. N.; Guedes da Silva,

M. F. C.; Pombeiro, A. J. L. Chalcogen Bonding in Synthesis, Catalysis and Design of Materials. *Dalton Trans.* **2017**, *46*, 10121–10138. (c) Beno, B. R.; Yeung, K. S.; Bartberger, M. D.; Pennington, L. D.; Meanwell, N. A. A Survey of the Role of Noncovalent Sulfur Interactions in Drug Design. *J. Med. Chem.* **2015**, *58*, 4383–438. (d) Huang, H.; Yang, L.; Facchetti, A.; Marks, T. J. Organic and Polymeric Semiconductors Enhanced by Noncovalent Conformational Locks. *Chem. Rev.* **2017**, *117*, 10291–10318. (e) Benz, S.; Besnard, C.; Matile, S. Chalcogen-Bonding Catalysis: From Neutral to Cationic Benzodiselenazole Scaffolds. *Helv. Chim. Acta* **2018**, *101*, e1800075. (f) Strakova, K.; Soleimanpour, S.; Diez-Castellnou, M.; Sakai, N.; Matile, S. Ganglioside-Selective Mechanosensitive Fluorescent Membrane Probes. *Helv. Chim. Acta* **2018**, *101*, e1800019. (g) Kremer, A.; Fermi, A.; Biot, N.; Wouters, J.; Bonifazi, D. Supramolecular Wiring of Benzo-1,3-Chalcogenazoles through Programmed Chalcogen Bonding Interactions. *Chem. Eur. J.* **2016**, *22*, 5665–5675. (h) Ho, P. C.; Szydlowski, P.; Sinclair, J.; Elder, P. J.; Kubel, J.; Gendy, C.; Lee, L. M.; Jenkins, H.; Britten, J. F.; Morim, D. R.; Vargas-Baca, I. Supramolecular Macrocycles Reversibly Assembled by Te(...)O Chalcogen Bonding. *Nat. Commun.* **2016**, *7*, 11299. (i) Garrett, G. E.; Gibson, G. L.; Straus, R. N.; Seferos, D. S.; Taylor, M. S. Chalcogen Bonding in Solution: Interactions of Benzotelluradiazoles with Anionic and Uncharged Lewis Bases. *J. Am. Chem. Soc.* **2015**, *137*, 4126–4133.

(11) Benz, S.; Poblador-Bahamonde Amalia, I.; Low-Ders, N.; Matile, S. Catalysis with Pnictogen, Chalcogen, and Halogen Bonds. *Angew. Chem. Int. Ed.* **2018**, *57*, 5408–5412.

(12) (a) Yang, M.; Tofan, D.; Chen, C.-H.; Jack, K. M.; Gabbaï, F. P. Digging the Sigma-Hole of Organoantimony Lewis Acids by Oxidation. *Angew. Chem. Int. Ed.* **2018**, *57*, 13868–13872. (b) Schmauck, J.; Breugst, M. The Potential of Pnicogen Bonding for Catalysis – a Computational Study. *Org. Biomol. Chem.* **2017**, *15*, 8037–8045. (c) Scheiner, S. Highly Selective Halide Receptors Based on Chalcogen, Pnicogen, and Tetrel Bonds. *Chem. Eur. J.* **2016**, *22*, 18850–18858. (d) Moaven, S.; Yu, J.; Vega, M.; Unruh, D. K.; Cozzolino, A. F. Self-Assembled Reversed Bilayers Directed by Pnictogen Bonding to Form Vesicles in Solution. *Chem. Commun.* **2018**, *54*, 8849-8852. (e) Christianson, A. M.; Gabbaï, F. P. A Lewis Acidic, π-Conjugated Stibaindole with a Colorimetric Response to Anion Binding at Sb(III). *Organometallics* **2017**, *36*, 3013-3015. (f) Kato, T.; Imoto, H.; Tanaka, S.; Ishidoshiro, M.; Naka, K. Facile Synthesis and Properties of Dithieno[3,2-b:2',3'-d]arsoles. *Dalton Trans*. **2016**, *45*, 11338–11345.

(13) Matile, S.; Sakai, N. "The Characterization of Synthetic Ion Channels and Pores," In Analytical Methods in Supramolecular Chemistry, C. Schalley (Ed), **2012**, 711–742.

(14) Wu, X.; Howe, E. N. W.; Gale, P. A. Supramolecular Transmembrane Anion Transport: New Assays and Insights. *Acc. Chem. Res.* **2018**, *51*, 1870–1879.

(15) Gale, P. A.; Davis, J. T.; Quesada, R. Anion Transport and Supramolecular Medicinal Chemistry. *Chem. Soc. Rev.* **2017**, *46*, 2497–2519.

(16) (a) Wang, D.-X.; Wang, M.-X. Anion−π Interactions: Generality, Binding Strength, and Structure. *J. Am. Chem. Soc.* **2013**, *135*, 892–897. (b) Watt, M. M.; Zakharov, L. N.; Haley, M. M.; Johnson, D. W. Selective Nitrate Binding in Competitive Hydrogen Bonding Solvents: Do Anion-pi Interactions Facilitate Nitrate Selectivity? *Angew. Chem. Int. Ed.* **2013**, *52*, 10275–10280. (c) Giese, M.; Albrecht, M.; Ivanova, G.; Valkonen, A.; Rissanen, K. Geometrically Diverse Anions in Anion–π Interactions. *Supramol. Chem.* **2012**, *24*, 48–55. (d) Adriaenssens, L.; Estarellas, C.; Vargas Jentzsch, A.; Martinez Belmonte, M.; Matile, S.; Ballester, P. Quantification of Nitrate−π Interactions and Selective Transport of Nitrate Using Calix[4]pyrroles with Two Aromatic Walls. *J. Am. Chem. Soc.* **2013**, *135*, 8324–8330. (e) Cotelle, Y.; Benz, S.; Avestro, A. J.; Ward, T. R.; Sakai, N.; Matile, S. Anion-pi Catalysis of Enolate Chemistry: Rigidified Leonard Turns as a General Motif to Run Reactions on Aromatic Surfaces. *Angew. Chem. Int. Ed.* **2016**, *55*, 4275–4279.

(17) He, Q.; Ao, Y. F.; Huang, Z. T.; Wang, D.-X. Self-Assembly and Disassembly of Vesicles as Controlled by Anion-pi Interactions. *Angew. Chem. Int. Ed.* **2015**, *54*, 11785–11790.

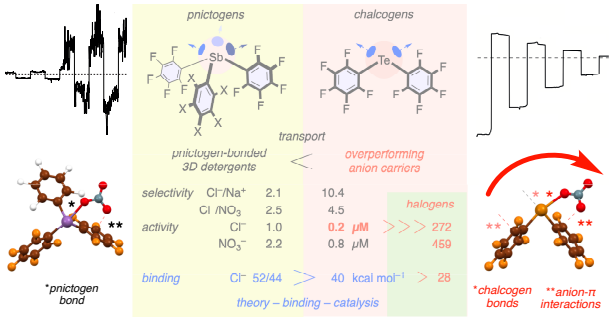
pnictogens
chalcogens
transport
pnictogen-bonded 3D detergents
overperforming anion carriers
selectivity Cl⁻/Na⁺ 2.1 10.4
Cl⁻/NO3⁻ 2.5 4.5
halogens
activity Cl⁻ 1.0 0.2 μM >>> 272
NO3⁻ 2.2 0.8 μM 159
binding Cl⁻ 52/44 > 40 kcal mol⁻¹ > 28
theory – binding – catalysis
*pnictogen bond
*chalcogen bonds
**anion-π interactions